Nanoscale

PAPER

View Article Online
View Journal | View Issue

Open Access Article. Published on 08 August 2016. Downloaded on 7/13/2024 7:51:44 PM.
This article is licensed under a Creative Commons Attribution-NonCommercial 3.0 Unported Licence.

Cite this: *Nanoscale*, 2016, **8**, 16044

Dramatic changes in DNA conductance with stretching: structural polymorphism at a critical extension†

Saientan Bag,[a] Santosh Mogurampelly,‡[a] William A. Goddard III[b,c] and Prabal K. Maiti*[a]

Received 27th April 2016,
Accepted 7th August 2016

DOI: 10.1039/c6nr03418g

www.rsc.org/nanoscale

In order to interpret recent experimental studies of the dependence of conductance of ds-DNA as the DNA is pulled from the 3′end1–3′end2 ends, which find a sharp conductance jump for a very short (4.5%) stretching length, we carried out multiscale modeling to predict the conductance of dsDNA as it is mechanically stretched to promote various structural polymorphisms. We calculate the current along the stretched DNA using a combination of molecular dynamics simulations, non-equilibrium pulling simulations, quantum mechanics calculations, and kinetic Monte Carlo simulations. For 5′end1–5′end2 attachments we find an abrupt jump in the current within a very short stretching length (6 Å or 17%) leading to a melted DNA state. In contrast, for 3′end1–3′end2 pulling it takes almost 32 Å (84%) of stretching to cause a similar jump in the current. Thus, we demonstrate that charge transport in DNA can occur over stretching lengths of several nanometers. We find that this unexpected behaviour in the B to S conformational DNA transition arises from highly inclined base pair geometries that result from this pulling protocol. We found that the dramatically different conductance behaviors for two different pulling protocols arise from how the hydrogen bonds of DNA base pairs break.

Introduction

Understanding how charge transport in dsDNA depends on its environment is important for designing such applications as bio-sensors or nanowires[1–5] and for understanding oxidative damage[6–11] and DNA repair. The charge transport properties of DNA have previously been reported to be that of an insulator,[12,13] a conductor,[14–16] a semiconductor, and even a superconductor.[17] This lack of reproducibility and the strong dependence on the external environment have made the subject of DNA conductance quite controversial. The charge transport in DNA is mediated by π–π stacking interaction (coupling) through its bases, which in turn is controlled by the rise and twist of the bases and by the external environment.[18–20] Consequently, to obtain reproducible DNA conductance measurements, the experiments necessarily require a reproducible electronic coupling between the bases, which is difficult to achieve experimentally.[21–23] Sophisticated single molecule experiments on DNA by Xu *et al.*,[19] Legrand *et al.*[24] and Song *et al.*[25] have concluded that[26] DNA is a semiconductor under ambient conditions. In ionic solutions in which DNA is able to keep its native state, DNA mainly exhibits semiconducting properties. In these experiments[19,24,25] the DNA was kept in an ionic environment between two electrodes and the current was measured either by scanning tunneling microscopy or by the break junction technique.

Extensive theoretical calculations have been reported on the charge transport of DNA. Cramer *et al.*[27] used the Marcus–Hush formalism to calculate the *I*–*V* characteristics of the DNA where the Marcus–Hush parameter was calculated using the extended Su–Schrieffer–Heeger Hamiltonian. Mallajosyula *et al.*[18] combined MD simulations using a force field with first principles quantum mechanics (QM) calculations to calculate the transmission coefficient for charge transport through DNA.

Recently, Tao *et al.*[28] studied the dependence of the conductance of ds-DNA as DNA is pulled from the 3′end1–3′end2 ends. They observed a sharp conductance jump for a very short (4.5%) stretching length, which they attributed to the breaking of hydrogen bonds between the terminal base-pairs at the DNA termini. In a related study, they compared the critical stretching

[a]*Center for Condensed Matter Theory, Department of Physics, Indian Institute of Science, Bangalore 560012, India. E-mail: maiti@physics.iisc.ernet.in*
[b]*IISc-DST Centenary Chair Professor, Department of Physics, Indian Institute of Science, Bangalore 560012, India*
[c]*Materials and Process Simulation Center, California Institute of Technology, Pasadena, California 91125, USA*
†Electronic supplementary information (ESI) available. See DOI: 10.1039/c6nr03418g
‡Present address: Department of Chemical Engineering, The University of Texas at Austin, Austin, Texas 78712, USA.

This journal is © The Royal Society of Chemistry 2016

Open Access Article. Published on 08 August 2016. Downloaded on 7/13/2024 7:51:44 PM.
This article is licensed under a Creative Commons Attribution-NonCommercial 3.0 Unported Licence.

length (the length at which the conduction jump occurs) of various closed-end and free end DNA systems.[29] Tao *et al.*[30] also studied the molecular conductance and piezoresistivity of dsDNA for various lengths and sequences. In a very recent study, Artés *et al.*[31] reported the increase in conductance of the DNA during its conformational change from B to A form.

In addition to the stretching of DNA from 3′end1–3′end2 as studied by Tao *et al.*, there are primarily three other modes to stretch DNA, leading to very different kinds of structures[32,33] depending on the stretching protocol. This raises the question of how the conductance in dsDNA depends on the mode of mechanical stretching.

In this paper we report a semiclassical Marcus–Hush type calculation of the charge transport through the dsDNA bases and present the current *vs*. stretching length behavior for each of the four pulling protocols considered in our simulations. Our calculations combine MD simulations, non-equilibrium pulling simulations, QM calculations, and kinetic Monte Carlo simulations. In all four cases, the jump in current was seen as the DNA is stretched but at different stretching lengths. The stretching length at which the jump in current occurs is defined as the critical stretching length l_c. For the case of 5′end1–5′end2 pulling, we found a short l_c of 6 Å, leading to a melted DNA state, while for 3′end1–3′end2 pulling, we found a high l_c of 32 Å, before the transformation from B to S-DNA. The l_c for the other two protocols (3′end1–5′end2 and 3′end1–5′end1) was found to have intermediate values.

The paper is organized as follows: in the next section we describe the all atom MD simulations and the non-equilibrium pulling simulations which were used to predict the structures arising from mechanical pulling. In the Methodology section we describe the Marcus–Hush formalism and the calculation scheme for the current through the DNA kept between two electrodes. The results are described in the section Results and discussion. In the section Summary and conclusion we summarize the results.

Simulation details

The initial structures of the duplex DNA was generated using the nucgen module available in the AMBER suite of[34] programs. We then simulated dsDNA with lengths of 12, 14, 16, 18 and 20 base pairs, using the following sequences:

- d(CGCGAATTCGCG),
- d(CGCGAAATTTCGCG),
- d(CGCGAAAATTTTCGCG),
- d(CGCGAAAAATTTTTCGCG) and
- d(CGCGAAAAAATTTTTTCGCG).

Each dsDNA structure was solvated in a box of water using a TIP3P water model. The water box dimensions were chosen to ensure 10 Å solvation of the dsDNA in each direction, when the DNA is fully stretched. Sufficient Na^+ counterions were added to neutralize the negative charge of phosphate backbone groups of the DNA. We followed the simulation protocol described in ref. 35 and 36 to equilibrate the system at a temperature of 300 K and a pressure of 1 bar. For constant force pulling simulations, we used modified-SANDER,[34] previously developed in our group,[37] to add the necessary forces at the dsDNA terminus. The external force was applied on the dsDNA using four different protocols as shown in Fig. 1. Starting from 0 pN, the external force increased linearly with time at the rate of 0.0001 pN fs^{-1}. The trajectory file was saved every 2 ps.

Methodology

The experimental situation that we want to mimic with our conductance calculations is shown schematically in Fig. 1(b). To measure the current through the dsDNA, we follow the semiclassical Marcus–Hush formalism[38,39] in which charge transport is described as incoherent hopping of charge carriers between dsDNA bases. In this formalism, the charge transfer

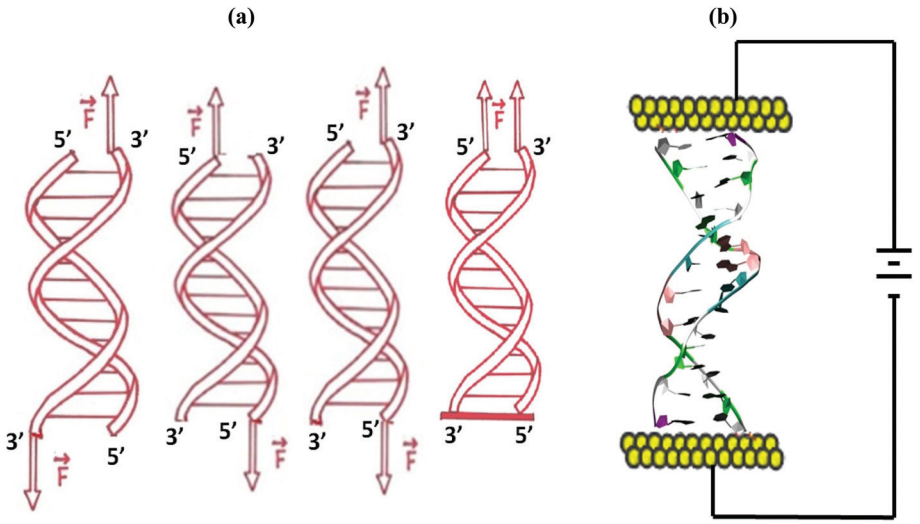

Fig. 1 (a) Schematic diagram of the forcing protocol for applying the force on the DNA. DNA is pulled from 3′end1–3′end2 ends, 5′end1–5′end2 ends, 3′end1–5′end2 ends and 3′end1–5′end1 ends. (b) Schematic diagram of the experimental situation that resembles our simulation.

Open Access Article. Published on 08 August 2016. Downloaded on 7/13/2024 7:51:44 PM.
This article is licensed under a Creative Commons Attribution-NonCommercial 3.0 Unported Licence.

rate ω_{ik} from the i^{th} charge hopping site to the k^{th} hopping site is given by

$$\omega_{ik} = \frac{|J_{ik}|^2}{\hbar}\sqrt{\frac{\pi}{\lambda k_B T}}\exp\left[-\frac{(\Delta G_{ik}-\lambda)^2}{4\lambda k_B T}\right] \quad (1)$$

where J_{ik} is the transfer integral, defined as

$$J_{ik} = \langle \phi^i|\hat{H}|\phi^k\rangle \quad (2)$$

Here ϕ^i and ϕ^k are the diabatic wave functions localized on the i^{th} and k^{th} sites, respectively. $\hat{H}$ is the Hamiltonian for the two site system between which the charge transfer takes place, ΔG_{ik} is the free energy difference between the two sites, λ is the reorganization energy, $\hbar$ is Planck's constant, k_B is the Boltzmann constant, and T is the absolute temperature.

In order to predict the dsDNA structures resulting from mechanical pulling, we performed non-equilibrium MD simulations as described in the previous section. Once the dsDNA structures are known, we remove the dsDNA backbone for additional calculations since we assume that the charge transport in DNA occurs solely through the interaction of the stacked bases. Previous theoretical and experimental investigation have demonstrated that the charge transport in DNA is mediated by stacked nucleobases through strong π–π interaction.[4,20,40,41] So we do not include the backbone during the optimization. Then we calculate[42–44] the charge transfer rates between the neighboring bases between which the charge transport takes place. For instance, if the electron is on the i^{th} base, the charge can hop to any one of its five neighboring bases (Fig. 2) requiring the calculation of five different hopping terms. With these rates in hand, we perform kinetic Monte Carlo simulations to obtain the numerical value for the current. We used Density Functional Theory (DFT) to calculate the various terms appearing in the rate expression. The highest occupied molecular orbital (HOMO) and the lowest unoccupied molecular orbital (LUMO) are used[45,46] as diabatic wave functions to calculate J between the pairs for hole and electron transport, respectively. Here $J = \langle \mathrm{HOMO}^i|\hat{H}|\mathrm{HOMO}^k\rangle$ and $J = \langle \mathrm{LUMO}^i|\hat{H}|\mathrm{LUMO}^k\rangle$ for hole and electron transport, respectively. We decompose the reorganization energy λ into two parts:

- inner sphere reorganization energy and
- outer sphere reorganization energy.

Inner sphere reorganization energy takes care of the change in nuclear degrees of freedom as charge transfer takes place from dsDNA base i to dsDNA base k, which we define as

$$\lambda_{ik}^{\mathrm{int}} = U_i^{\mathrm{nC}} - U_i^{\mathrm{nN}} + U_k^{\mathrm{cN}} - U_k^{\mathrm{cC}} \quad (3)$$

where U_i^{nC} (U_i^{cN}) is the internal energy of a neutral (charged) base in charged (neutral) state geometry and U_i^{nN} (U_i^{cC}) is the internal energy of a neutral (charged) base in neutral (charged) state geometry. To calculate the terms appearing in eqn (3), we first optimized the geometry of hopping sites for both neutral and charged states using Gaussian09.[47] Then we carried out single point energy calculations with the optimized geometry for these different charged states to obtain various terms involved in the internal reorganization energy appearing in eqn (3).

The outer sphere reorganization energy is the part of the reorganization energy that takes into account the reorganization of the environment as charge transfer takes place. The calculation of external reorganization energy is very involved and intricate.[43] In our calculations, we take the external reorganization as a parameter, rather than calculating it from the QM. The free energy difference ΔG_{ik} appearing in the rate expression is the contribution from various sources as described below:

$$\Delta G_{ik} = \Delta G_{ik}^{\mathrm{ext}} + \Delta G_{ik}^{\mathrm{int}} \quad (4)$$

Here $\Delta G_{ik}^{\mathrm{ext}}$ is the contribution from the external electric field, defined as $\Delta G_{ik}^{\mathrm{ext}} = F\cdot d_{ik}$, where F is the applied electric field and d_{ik} is the relative position vector between the i^{th} and k^{th} bases. In our case this expression simplifies to the following:

$$\begin{aligned}\Delta G_{ik}^{\mathrm{ext}} &= \frac{V}{N} \quad \text{for relative position of } i^{th} \text{ and } k^{th} \text{ bases as shown in Fig. 2(a)}\\ &= 0 \quad \text{for relative position of } i^{th} \text{ and } k^{th} \text{ bases as shown in Fig. 2(b)}\\ &= -\frac{V}{N} \quad \text{for relative position of } i^{th} \text{ and } k^{th} \text{ bases as shown in Fig. 2(c).}\end{aligned}$$

Here V is the applied voltage and N is the number of base-pairs. $\Delta G_{ik}^{\mathrm{int}}$ is the contribution in free energy differ-

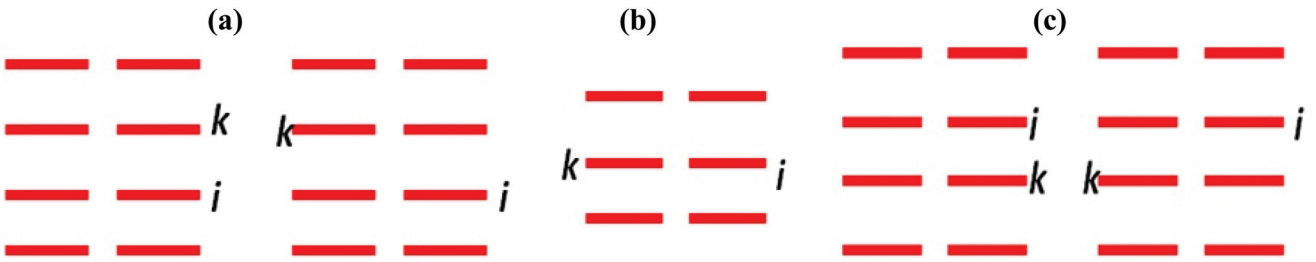

Fig. 2 Schematic representation of the relative positions of the charge hopping pairs (DNA bases) in the experimental situation described in Fig. 1(b). If charge is on site i, it can hop upwards to site k (a), to site k in the same plane (b) or downwards to site k (c).

 This journal is © The Royal Society of Chemistry 2016

Open Access Article. Published on 08 August 2016. Downloaded on 7/13/2024 7:51:44 PM.
This article is licensed under a Creative Commons Attribution-NonCommercial 3.0 Unported Licence.

ence due to different internal energies, which can be written as

$$\Delta G_{ik}^{\text{int}} = U_i^{\text{cC}} - U_i^{\text{nN}} + U_k^{\text{cC}} - U_k^{\text{nN}} \quad (5)$$

where U_i^{cC} (U_i^{nN}) is the internal energy of base i in the charged (neutral) state and geometry. We calculated ω_{ik} for all hopping pairs and simulate the charge transport dynamics using the kinetic Monte Carlo (MC) method.

We emphasize here that we have only calculated the charge transport rates between the bases, whereas to completely simulate the experimental situation one should also calculate the rates between the base and the electrode. We have not explicitly calculated these rates. The explicit calculation scheme for these rates can be found in an article by Rosa Di Felice's group.[48] These rates are chosen such that the calculated conductivity becomes independent of these rates (see ESI section I†). Consequently, the conductivity that we report here is expected to correspond to the intrinsic conductivity of the DNA.

For kinetic MC, we developed a code[44] with the following algorithm. We assign a unit positive charge (for hole transport) or negative charge (electron transport) to any hopping site i. At this point we initialize the time as $t = 0$. If site i has N neighbours, then the waiting time τ for the charge is calculated according to the equation:

$$\tau = -\omega_i^{-1} \ln(r_1) \quad \left[\omega_i = \sum_{k=1}^{N} \omega_{ik}\right] \quad (6)$$

and time is updated as $t = t + \tau$. Here k is the index of the neighbours (the hopping sites to which the charge can hop) coupled to the particular hopping site i and r_1 is a uniform random number between 0 and 1. To decide where the charge will hop among N neighbours, we chose the largest k for which $\frac{\sum_k \omega_{ik}}{\omega_i} \leq r_2$. Here k is the index of the neighbours of site i and r_2 is another uniform random number between 0 and 1. The above condition will ensure that the side k is selected with probability $\frac{\omega_{ik}}{\omega_i}$. Next the position of the charge is updated and the above process is repeated. The current through the DNA is calculated as follows:

$$I = e\langle v \rangle = e\langle l \rangle / t$$

$\langle v \rangle$ is the average velocity of the charge and $\langle l \rangle$ is the average distance that the charge has moved in time t.

Results and discussion

All the DFT calculations mentioned in the previous section used the M06-2X/6-311G level of theory as implemented in the Gaussian 09 package. To validate the methodological scheme described in the previous section, we first calculated the resistance of the dsDNA as a function of dsDNA length at an applied voltage of 5 V, and the corresponding results are displayed in Fig. 3. The resistance as a function of dsDNA length for 1 V and 6 V applied voltages are shown in Fig. S4 of the ESI.† The resistance increases almost linearly with the length of the dsDNA as has been observed experimentally.[28] This increase of resistance with molecular length is an essential feature of the thermally activated hopping (Marcus–Hush) mechanism. Next we calculate the current at an applied voltage of 5 V through all stretched DNA structures starting from the unstretched one for the 5′end1–5′end2 case. The reference voltage of 5 V was chosen because the current through the unstretched dsDNA saturates above 5 V (see ESI section II†). We found that the current exhibits a sharp jump (Fig. 4(a)) beyond a critical stretching length of 6 Å, as reported by Tao *et al.*[28] at which point the conductance drops by 3 orders of magnitude. We note here that to include the effect of solvation of the dsDNA in the conductance calculation, we treated the surrounding water medium using a polarizable continuum model[49] (PCM) with a static dielectric constant of 78.3 and a dynamic dielectric constant of 1.77. To validate the accuracy of this calculation, we also carried out the current calculations using the B3LYP/6-311G level of theory and found a similar conductance jump of 4.1×10^{-8} A V^{-1} rather than 2.8×10^{-8} A V^{-1} (see Fig. S3 of the ESI†). It is important to note that without the solvation effect, we do not get the sharp conductance jump shown in Fig. S3 of the ESI.†

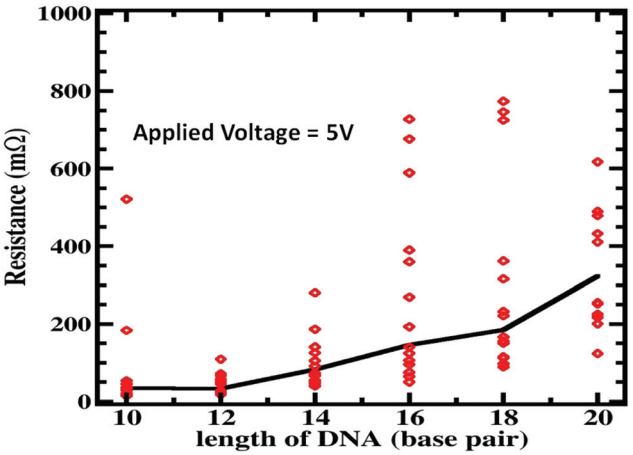

Fig. 3 Resistance of the dsDNA with increasing length. The red points indicate the individual case studied and a mean line is drawn to guide the eyes. The resistance increases almost linearly with the length of the DNA. This increase of resistance with molecular length, which was also observed in the experiment, is an essential feature of the thermally activated hopping (Marcus) mechanism.

Next we calculate the current as a function of stretching length for the other three pulling protocols using the same level of theory and the solvation model as for the 5′end1–5′end2 case presented in the previous paragraph. Here we emphasize the complexity of the current calculations presented in this work. We calculated the current through almost 200 dsDNA structures for the 5′end1–5′end2 case while we calculated the current through 600, 300, and 400 dsDNA

Open Access Article. Published on 08 August 2016. Downloaded on 7/13/2024 7:51:44 PM.
This article is licensed under a Creative Commons Attribution-NonCommercial 3.0 Unported Licence.

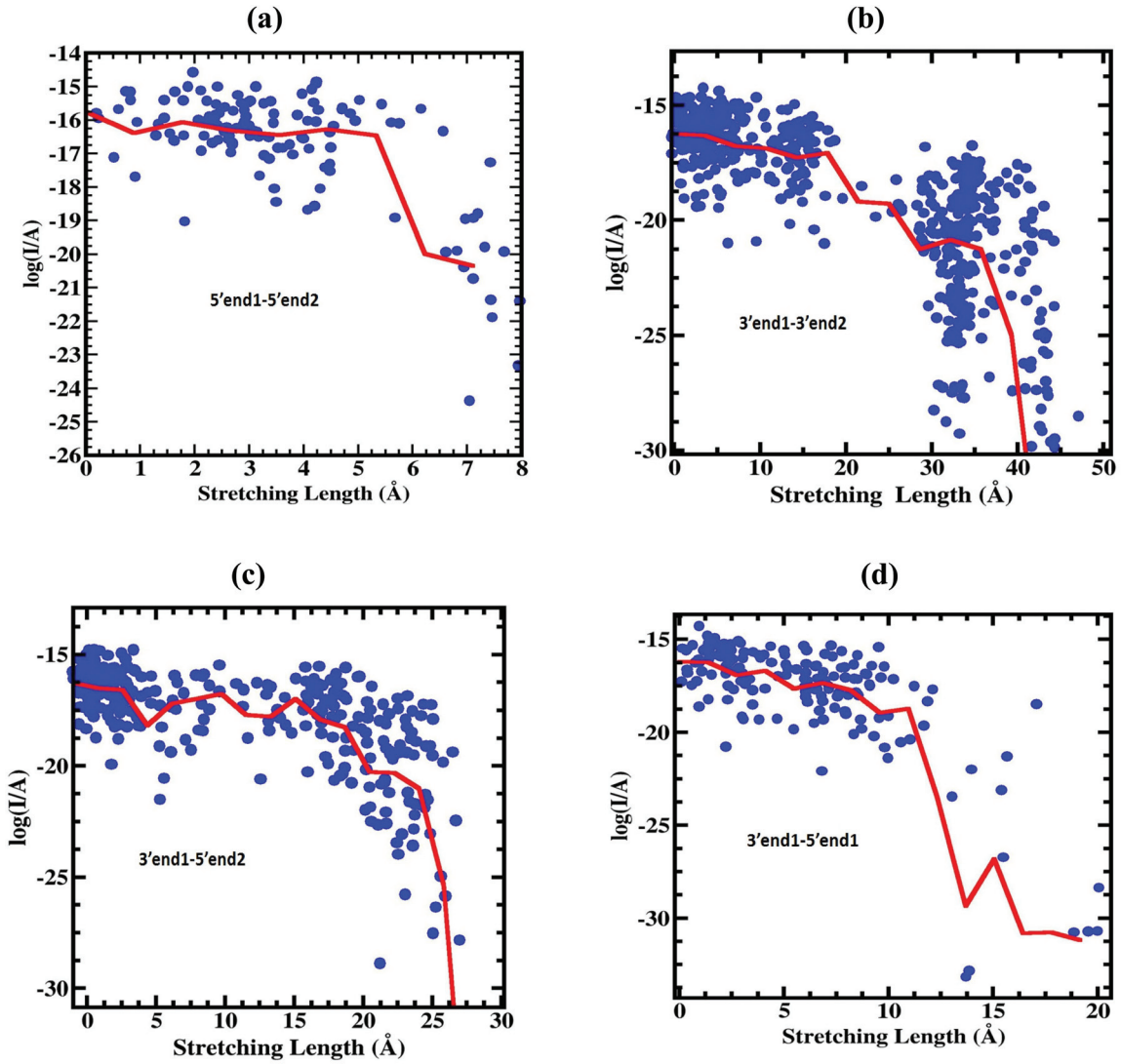

Fig. 4 Current through the DNA as a function of the stretching length for pulling from 5′end1–5′end2 ends (a), 3′end1–3′end2 ends (b), 3′end1–5′end2 ends (c) and 3′end1–5′end1 ends (d). The actual values of current for all individual cases studied are shown in blue dots. A mean line in red is drawn to guide the eyes.

structures for the 3′end1–3′end2, 3′end1–5′end2, and 3′end1–5′end1 cases, respectively. The jump in current was seen for all four cases but at different stretching lengths (Fig. 4). Table 1 tabulates the numerical value critical stretching length l_c for the various pulling protocols. A high critical stretching length (32 Å) was found for the 3′end1–3′end2 case, but it was very short (6 Å) for the 5′end1–5′end2 case.

Table 1 Numerical value of the critical stretching length (l_c) for various pulling protocols

Pulling protocol	l_c (Å)
5′end1–5′end2	6 ± 1
3′end1–3′end2	32 ± 5
3′end1–5′end2	23 ± 2
3′end1–5′end1	11.25 ± 2

To extract a molecular level understanding of the pulling protocol dependent conductance behavior, we now examine the dsDNA structures at various stretching lengths for the various pulling protocols. Since the external environment to the dsDNA does not change during the mechanical pulling, the decay in conductance jump can be ascribed to the structural changes in DNA structures, which in turn affect the rate equation. Several instantaneous snapshots of the dsDNA resulting from the pulling simulations are shown in Fig. 5. This shows a clear indication of different structures appearing for different pulling cases. As a quantitative measure of the structural changes, we calculate the number of intact hydrogen bonds as a function of the applied force for all four cases (Fig. 6). In the 5′end1–5′end2 and 3′end1–5′end1 modes, all H-bonds are cleaved within a force of ~600 pN, leading to a melted DNA state while 80% H-bond retention is observed for

 This journal is © The Royal Society of Chemistry 2016

Open Access Article. Published on 08 August 2016. Downloaded on 7/13/2024 7:51:44 PM.
This article is licensed under a Creative Commons Attribution-NonCommercial 3.0 Unported Licence.

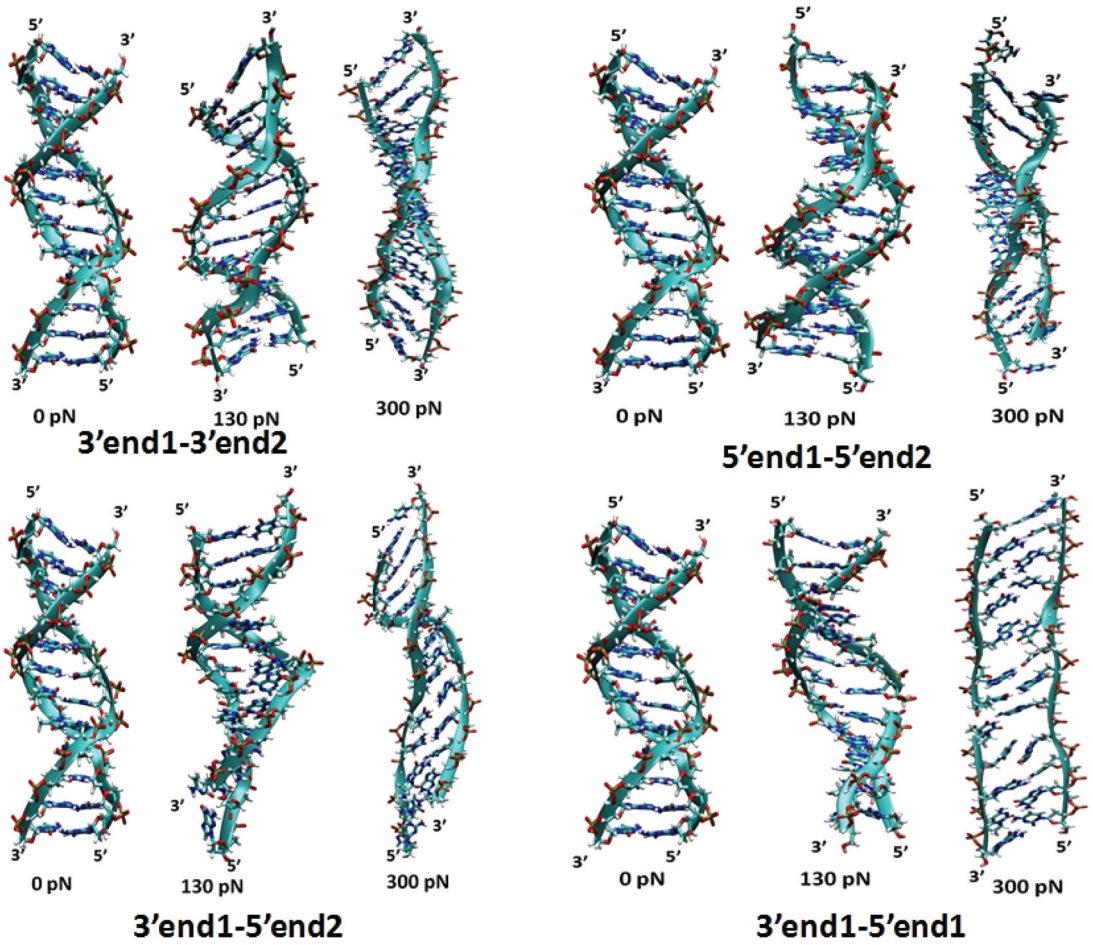

Fig. 5 Instantaneous snapshot of the DNA with increasing pulling forces for pulling 3′end1–3′end2 ends, 5′end1–5′end2 ends, 3′end1–5′end2 ends and 3′end1–5′end1 ends respectively.

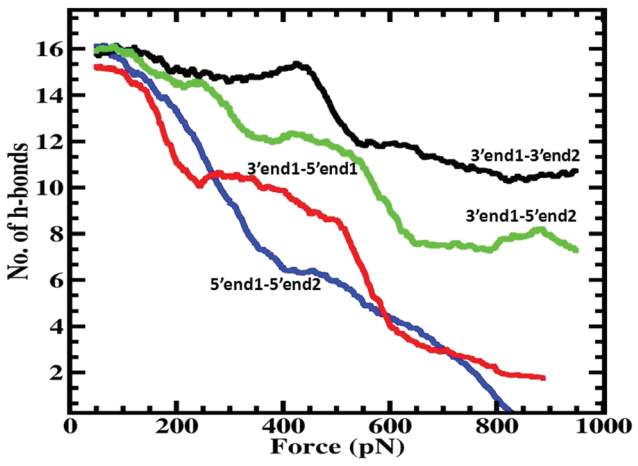

Fig. 6 Number of hydrogen bonds as a function of applied force on DNA for 5′end1–5′end2 and 3′end1–3′end2, 3′end1–5′end1 and 3′end1–5′end2 pulling cases. In the case of 5′end1–5′end2 and 3′end1–5′end1 pulling all hydrogen-bonds get cleaved within ~600 pN force, indicating a melted DNA state, while 80% H-bonds remain intact for 3′end1–3′end2 pulling cases, which indicates B–S structural transition of the DNA. The 3′end1–5′end2 pulling case is intermediate of these two extreme situations.

the 3′end1–3′end2 mode, indicating the B–S structural transition of the DNA. The 3′end1–5′end2 pulling case is intermediate of these two extreme situations. To further investigate how the structural change modifies the hopping rate, we first identified the defects (shown by the red circle in Fig. 7) that appear in the dsDNA during the course of mechanical pulling and plot the transfer integral (Fig. 7) between the corresponding bases in the region of defect. We also show the changes in the total number of intact hydrogen bonds (Fig. 7) between the base-pairs as the defect in the dsDNA appears for all four pulling protocols. It is clear from Fig. 7 that for all the four different pulling protocols, the creation of a defect causes a sharp reduction of the transfer integral which in turn affects the charge transfer rate, resulting in the sharp attenuation of the current. The appearance of the defect can be associated with the change in the total number of hydrogen-bonds. The reason behind this dramatic difference in stretching length for the 5′end1–5′end2 pulling and 3′end1–3′end2 pulling is that the structure of the dsDNA stretched from 3′end1–3′end2 ends dramatically differs from the structure stretched from 5′end1–5′end2 ends.[33] This difference in structure arising from 3′end1–3′end2 pulling and 5′end1–5′end2 pulling can also be

Open Access Article. Published on 08 August 2016. Downloaded on 7/13/2024 7:51:44 PM.
This article is licensed under a Creative Commons Attribution-NonCommercial 3.0 Unported Licence.

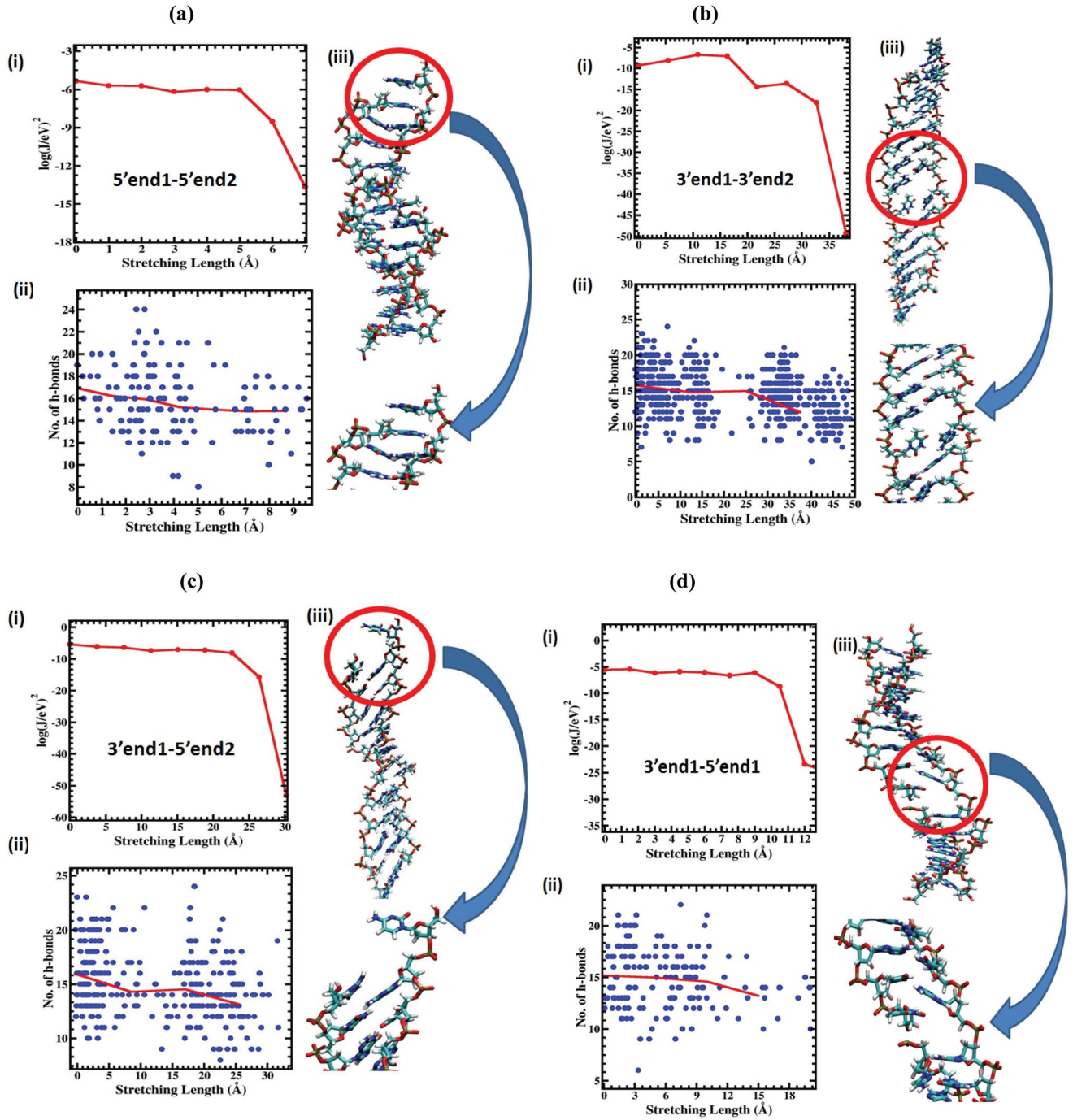

Fig. 7 (i) Transfer integral as a function of stretching length. (ii) Number of H-bonds as a function of stretching length. Blue dots are the number of individual cases and the red line is the average. (iii) Instantaneous snapshots of the dsDNA showing the appearance of defects due to the breaking of H-bonds in the course of mechanical pulling: (a) 5′end1–5′end2′ case, (b) 3′end1–3′end2 case, (c) 3′end1–5′end2 case and (d) 3′end1–5′end1 case. Appearance of the defect is associated with the sharp reduction in transfer integral and the change in the total number of H-bonds.

understood by plotting the inclination angle as a function of applied force (see Fig. S5 of the ESI†). Initially the DNA is in B form where the base pairs are tilted with respect to the global axis of the dsDNA.[33] As one stretches the DNA from 5′end1–5′end2 ends, this tilt gets increased, which causes the breakage of terminal H-bond resulting in the early conductance jump. On the other hand, the 3′end1–3′end2 pulling decreases the base pair tilt. As a result no early breakage of H-bond occurs, rather the DNA undergoes structural transformation from B to S form.

The calculation of the current through the DNA was carried out assuming that the charge transport through the DNA

 This journal is © The Royal Society of Chemistry 2016

Open Access Article. Published on 08 August 2016. Downloaded on 7/13/2024 7:51:44 PM.
This article is licensed under a Creative Commons Attribution-NonCommercial 3.0 Unported Licence.

happens *via* incoherent hopping of charge through the bases. Since the DNA we have studied is short in length (12 bp), the transport of charge will have also a contribution from tunneling.[50,51] However the main conclusions (critical stretching length) of the paper remain and do not change due to the inclusion of tunneling (see section X of the ESI†).

The stretching length *vs.* current calculation described above was performed at 300 K. To understand the effect of temperature on the dynamics we also calculated the response for 5′end1–5′end2 pulling at 350 K and 250 K. The H-bond profiles are shown in Fig. S7(a) of the ESI.† The dependence of the number of H-bonds as a function of force is similar at all three temperatures but we found faster H-bond decay with force at higher temperature. However, the conductance jump at 6 Å remains largely unaffected by the temperature as shown in Fig. S7(b) of the ESI.† These results that the decrease in H-bonds with force is faster at high temperatures suggest that there is an activation process involving a barrier of 0.114 eV,[52] whereas the temperature independence of the transition at 6 Å length suggests that this may be geometrically related to the stiff bonds of the system.

The high voltage of 5 V was chosen from the experimental *V–I* characteristics of the DNA, where it is observed that the current saturates at high voltage. At low voltage the current will be low but the behavior of stretching length *vs.* current plot does not change. To demonstrate this, we report in Fig. S8 of the ESI† the current *vs.* stretching length for bias voltages of 1 V and 0.5 V. The critical stretching length does not change at the smaller bias, but of course the current is lower.

Our calculations have assumed that the external reorganization energy is zero. However introducing the external reorganization energy would not affect the behavior of current as a function of end-to-end length of the dsDNA; it only reduces the total magnitude of the current (see ESI section VI†).

All the calculations reported in this section are for a specific sequence of the DNA. In order to show that the structural changes of the dsDNA (which are responsible for the conductance jump) for various pulling protocols do not depend significantly on the specific sequence of the DNA, we carried out studies for two other dramatically different sequences. As shown in section IX (Fig. S9†) of the ESI,† the different sequences lead to the same structural patterns with pulling. Thus we expect the results reported to be independent of the specific DNA sequence.

Summary and conclusion

In summary, we have predicted the behaviour of current through dsDNA molecules kept between two electrodes as we stretch the molecule mechanically using four different protocols. Our calculation of current is based on the thermally activated hopping mechanism, which takes into account a very realistic description of DNA structures and of the external environment of the DNA. We found that the response of current through DNA under mechanical pulling depends strongly on the pulling mechanism. We found an abrupt jump in current of almost three orders of magnitude within a very short stretching length (6 Å) in the case of 5′end1–5′end2 pulling while in the case of 3′end1–3′end2 pulling it takes almost 32 Å of stretching (84%) to observe a similar jump in current. We demonstrate that this change of current is associated with the change of the transfer integral J_{ik}, which is manifested by the structural changes of DNA.

Thus these calculations provide an atomistic understanding of the behavior of DNA conductance under mechanical tension. These results further explain the piezoresistive behavior[30] of DNA, which is an important property for its application in nanodevices. The point at which there is a jump in conductance as a function of stretching will also help in developing a DNA based mechanical switch.[53] We expect that these calculations should help further development of DNA nanotechnology.

Acknowledgements

We thank DST, India for financial support. We thank Dr Andres Jaramillo-Botero for helpful discussions. Support for WAG was from NSF EFRI-1332411.

References

1 C. R. Treadway, M. G. Hill and J. K. Barton, *Chem. Phys.*, 2002, **281**, 409–428.
2 S. Delaney and J. K. Barton, *J. Org. Chem.*, 2003, **68**, 6475–6483.
3 G. B. Schuster, *Long-range charge transfer in DNA II*, Springer Science & Business Media, 2004.
4 R. Endres, D. Cox and R. Singh, *Rev. Mod. Phys.*, 2004, **76**, 195.
5 D. Porath, G. Cuniberti and R. Di Felice, in *Long-Range Charge Transfer in DNA II*, Springer, 2004, pp. 183–228.
6 D. B. Hall, R. E. Holmlin and J. K. Barton, *Nature*, 1996, **382**, 731–735.
7 D. Ly, L. Sanii and G. B. Schuster, *J. Am. Chem. Soc.*, 1999, **121**, 9400–9410.
8 E. Meggers, D. Kusch, M. Spichty, U. Wille and B. Giese, *Angew. Chem., Int. Ed.*, 1998, **37**, 460–462.
9 I. Saito, T. Nakamura, K. Nakatani, Y. Yoshioka, K. Yamaguchi and H. Sugiyama, *J. Am. Chem. Soc.*, 1998, **120**, 12686–12687.
10 B. Armitage, *Chem. Rev.*, 1998, **98**, 1171–1200.
11 S. O. Kelley and J. K. Barton, *Science*, 1999, **283**, 375–381.
12 P. De Pablo, F. Moreno-Herrero, J. Colchero, J. G. Herrero, P. Herrero, A. Baró, P. Ordejón, J. M. Soler and E. Artacho, *Phys. Rev. Lett.*, 2000, **85**, 4992.
13 Y. Zhang, R. Austin, J. Kraeft, E. Cox and N. Ong, *Phys. Rev. Lett.*, 2002, **89**, 198102.
14 H. Fink and C. Schönenberger, *Nature*, 1999, **398**, 407–410.
15 D. Porath, A. Bezryadin, S. De Vries and C. Dekker, *Nature*, 2000, **403**, 635–638.

Open Access Article. Published on 08 August 2016. Downloaded on 7/13/2024 7:51:44 PM.
This article is licensed under a Creative Commons Attribution-NonCommercial 3.0 Unported Licence.

16 K. H. Yoo, D. H. Ha, J. O. Lee, J. W. Park, J. Kim, J. J. Kim, H. Y. Lee, T. Kawai and H. Y. Choi, *Phys. Rev. Lett.*, 2001, **87**, 198102.
17 A. Y. Kasumov, M. Kociak, S. Gueron, B. Reulet, V. Volkov, D. Klinov and H. Bouchiat, *Science*, 2001, **291**, 280–282.
18 S. S. Mallajosyula, J. C. Lin, D. L. Cox, S. K. Pati and R. R. P. Singh, *Phys. Rev. Lett.*, 2008, **101**, 176805.
19 B. Xu, P. M. Zhang, X. L. Li and N. J. Tao, *Nano Lett.*, 2004, **4**, 1105–1108.
20 R. Venkatramani, S. Keinan, A. Balaeff and D. N. Beratan, *Coord. Chem. Rev.*, 2011, **255**, 635–648.
21 X. Cui, A. Primak, X. Zarate, J. Tomfohr, O. Sankey, A. Moore, T. Moore, D. Gust, G. Harris and S. Lindsay, *Science*, 2001, **294**, 571–574.
22 M. Magoga and C. Joachim, *Phys. Rev. B: Solid State*, 1997, **56**, 4722.
23 F. Moresco, L. Gross, M. Alemani, K. H. Rieder, H. Tang, A. Gourdon and C. Joachim, *Phys. Rev. Lett.*, 2003, **91**, 036601.
24 O. Legrand, D. Côte and U. Bockelmann, *Phys. Rev. E: Stat. Phys., Plasmas, Fluids, Relat. Interdiscip. Top.*, 2006, **73**, 031925.
25 B. Song, M. Elstner and G. Cuniberti, *Nano Lett.*, 2008, **8**, 3217–3220.
26 M. Wolter, P. B. Woiczikowski, M. Elstner and T. Kubař, *Phys. Rev. B: Condens. Matter*, 2012, **85**, 075101.
27 T. Cramer, S. Krapf and T. Koslowski, *J. Phys. Chem. C*, 2007, **111**, 8105–8110.
28 C. Bruot, L. Xiang, J. L. Palma and N. Tao, *ACS Nano*, 2015, **9**, 88–94.
29 C. Bruot, L. Xiang, J. L. Palma, Y. Li and N. Tao, *J. Am. Chem. Soc.*, 2015, **137**, 13933–13937.
30 C. Bruot, J. L. Palma, L. Xiang, V. Mujica, M. A. Ratner and N. Tao, *Nat. Commun.*, 2015, **6**, 8032.
31 J. M. Artés, Y. Li, J. Qi, M. Anantram and J. Hihath, *Nat. Commun.*, 2015, **6**, 8870.
32 A. Lebrun and R. Lavery, *Nucleic Acids Res.*, 1996, **24**, 2260–2267.
33 C. Danilowicz, C. Limouse, K. Hatch, A. Conover, V. W. Coljee, N. Kleckner and M. Prentiss, *Proc. Natl. Acad. Sci. U. S. A.*, 2009, **106**, 13196–13201.
34 D. A. Pearlman, D. A. Case, J. W. Caldwell, W. S. Ross, T. E. Cheatham, S. DeBolt, D. Ferguson, G. Seibel and P. Kollman, *Comput. Phys. Commun.*, 1995, **91**, 1–41.
35 P. K. Maiti, T. A. Pascal, N. Vaidehi and W. A. Goddard, *Nucleic Acids Res.*, 2004, **32**, 6047–6056.
36 P. K. Maiti and B. Bagchi, *Nano Lett.*, 2006, **6**, 2478–2485.
37 M. Santosh and P. K. Maiti, *J. Phys.: Condens. Matter*, 2009, **21**, 034113.
38 R. A. Marcus, *Rev. Mod. Phys.*, 1993, **65**, 599.
39 W. Q. Deng, L. Sun, J. D. Huang, S. Chai, S. H. Wen and K. L. Han, *Nat. Protoc.*, 2015, **10**, 632–642.
40 S. Priyadarshy, S. M. Risser and D. N. Beratan, *J. Biol. Inorg. Chem.*, 1998, **3**, 196–200.
41 S. O. Kelley, E. M. Boon, J. K. Barton, N. M. Jackson and M. G. Hill, *Nucleic Acids Res.*, 1999, **27**, 4830–4837.
42 J. Kirkpatrick, V. Marcon, J. Nelson, K. Kremer and D. Andrienko, *Phys. Rev. Lett.*, 2007, **98**, 227402.
43 V. Rühle, A. Lukyanov, F. May, M. Schrader, T. Vehoff, J. Kirkpatrick, B. Baumeier and D. Andrienko, *J. Chem. Theory Comput.*, 2011, **7**, 3335–3345.
44 S. Bag, V. Maingi, P. K. Maiti, J. Yelk, M. A. Glaser, D. M. Walba and N. A. Clark, *J. Chem. Phys.*, 2015, **143**, 144505.
45 P. Borsenberger, L. Pautmeier and H. Bässler, *J. Chem. Phys.*, 1991, **94**, 5447–5454.
46 M. D. Newton, *Chem. Rev.*, 1991, **91**, 767–792.
47 M. Frisch, G. Trucks, H. B. Schlegel, G. Scuseria, M. Robb, J. Cheeseman, G. Scalmani, V. Barone, B. Mennucci and G. E. Petersson, *Gaussian 09*, 2009.
48 W. Sun, A. Ferretti, D. Varsano, G. Brancolini, S. Corni and R. Di Felice, *J. Phys. Chem. C*, 2014, **118**, 18820–18828.
49 J. Tomasi, B. Mennucci and R. Cammi, *Chem. Rev.*, 2005, **105**, 2999–3094.
50 B. Giese, J. Amaudrut, A.-K. Köhler, M. Spormann and S. Wessely, *Nature*, 2001, **412**, 318–320.
51 G. Li, N. Govind, M. A. Ratner, C. J. Cramer and L. Gagliardi, *J. Phys. Chem. Lett.*, 2015, **6**, 4889–4897.
52 S. Mogurampelly, S. Panigrahi, D. Bhattacharyya, A. Sood and P. K. Maiti, *J. Chem. Phys.*, 2012, **137**, 054903.
53 D. Řeha, A. A. Voityuk and S. A. Harris, *ACS Nano*, 2010, **4**, 5737–5742.

This journal is © The Royal Society of Chemistry 2016